

Durability of VEGF Suppression With Intravitreal Aflibercept and Brolucizumab: Using Pharmacokinetic Modeling to Understand Clinical Outcomes

Thomas Eissing¹, Michael W. Stewart², Cynthia X. Qian³, and Kay D. Rittenhouse⁴

¹ Clinical Pharmacometrics, Bayer AG, Leverkusen, Germany

² Department of Ophthalmology, Mayo Clinic College of Medicine, Jacksonville, FL, USA

³ Department of Ophthalmology, University of Montreal, Montreal, Canada

⁴ Medical Affairs Ophthalmology, Bayer Consumer Care AG, Basel, Switzerland

Correspondence: Kay D. Rittenhouse, Medical Affairs Ophthalmology, Bayer Consumer Care AG, Peter Merian-Strasse 84, CH-4052 Basel, Switzerland. e-mail: kay.rittenhouse@bayer.com

Received: October 19, 2020

Accepted: February 26, 2021

Published: April 13, 2021

Keywords: aflibercept; brolucizumab; vascular endothelial growth factor; pharmacokinetic-pharmacodynamic analysis; age-related macular degeneration

Citation: Eissing T, Stewart MW, Qian CX, Rittenhouse KD. Durability of VEGF suppression with intravitreal aflibercept and brolucizumab: Using pharmacokinetic modeling to understand clinical outcomes. *Trans Vis Sci Tech.* 2021;10(4):9. <https://doi.org/10.1167/tvst.10.4.9>

Purpose: To investigate whether vascular endothelial growth factor (VEGF)-suppression durations contribute to our understanding of clinical trial outcomes by simulating vitreous molar concentrations (C_{vm}) of intravitreal aflibercept (IVT-AFL) and brolucizumab (IVT-BRO) using pharmacokinetic (PK) modeling.

Methods: A PK model simulated C_{vm} after single-dose IVT-AFL, IVT-BRO, and ranibizumab (IVT-RAN), and extrapolated intraocular VEGF-suppression thresholds and durations. Vitreous PK after multidose regimens used in studies of IVT-AFL versus IVT-BRO were simulated and compared with best-corrected visual acuity (BCVA) data.

Results: C_{vm} peaked higher (C_{max}) and decreased more quickly to the VEGF-suppression threshold and minimum (C_{min}) levels with IVT-BRO than with IVT-AFL, consistent with their molar doses calculated using molecular weights and vitreous half-lives (26 kDa and 115 kDa; 4.4–5.1 and 9.1–11 days, respectively). The mean VEGF suppression durations were 71 days for IVT-AFL 2 mg and 51 (48–59) days for IVT-BRO 6 mg. Based on dosing in OSPREY (matched dosing to week [w]32 for both agents; thereafter, IVT-AFL every eight weeks [q8w] and IVT-BRO q12w for the last two doses [w32→w44 and w44→w56]), IVT-BRO showed wider C_{max} – C_{min} fluctuations than IVT-AFL. The IVT-BRO C_{min} fell below the VEGF-suppression threshold at timepoints near w56, when decreases in BCVA were also observed. The IVT-AFL vitreous C_{min} remained above the suppression threshold through w56, where BCVA gains were maintained.

Conclusions: The PK-modeled mean VEGF-suppression duration for IVT-BRO was substantially shorter than that published for IVT-AFL and may not be sufficient to effectively suppress VEGF throughout q12w dosing.

Translational Relevance: The PK modeling suggests that more patients may be maintained on ≥q12w dosing with IVT-AFL than with IVT-BRO.

Introduction

Natural vascular endothelial growth factor (VEGF) signaling is enhanced to a pathophysiological level in patients with retinal and choroidal vascular permeability and neovascular disorders.¹ In these patients, anti-VEGF treatments attenuate excessive VEGF signaling by preventing binding of VEGF to receptors.^{2–4} Because VEGF is constantly synthesized, deleteri-

ous levels recur when anti-VEGF drug concentrations decrease.⁵ Therefore, to mitigate the treatment burden associated with intravitreal dosing of anti-VEGF agents, research has focused on identifying agents with molecular features and pharmacokinetic (PK) and pharmacodynamic (PD) properties that facilitate optimal dosing regimens (with reduced injection frequency and treatment burden) by maintaining VEGF suppression and optimizing overall treatment outcomes.⁶

PK principles are important in optimizing dosing regimens. In contrast with systemic routes of drug delivery in which PK and PD have been comprehensively characterized, the challenges of obtaining regular or frequent samples of vitreous or aqueous ocular fluids have limited the number of studies that evaluate intraocular (especially vitreous) PK. PK/PD modeling integrates known pharmacology and kinetics of drugs using the limited data available to improve prediction of clinical response to intravitreal anti-VEGF drugs. PK characteristics are also relevant for achieving and maintaining target concentrations within the posterior segment of the eye after intravitreal injection and are driven by the molecular features of the agents.

Intravitreal aflibercept (IVT-AFL) is a recombinant fusion protein consisting of portions of human VEGF receptors 1 and 2 extracellular domains fused to the fragment crystallizable (Fc) portion of the human immunoglobulin G1 (IgG1) antibody that binds VEGF-A, VEGF-B, and placental growth factor.² Intravitreal ranibizumab (IVT-RAN) is a humanized monoclonal IgG1 kappa isotype antibody fragment (Fab) that binds VEGF-A and lacks an Fc region.⁴ Intravitreal brolucizumab (IVT-BRO) is a humanized monoclonal single-chain variable domain antibody fragment (SCFv), which also lacks an Fc region and binds VEGF-A.³ The binding affinities for VEGF₁₆₅ are ranked IVT-AFL > IVT-BRO > IVT-RAN.^{7,8}

Intravitreal anti-VEGF dosing produces vitreous drug concentrations that far exceed VEGF levels within the vitreous.^{5,9} Thus initial PD effects are driven by the duration of time the drug concentrations remain above the minimum required to inhibit VEGF, that is, the minimum inhibitory concentration or “VEGF-suppression thresholds.” The VEGF-suppression threshold itself is dependent on target binding affinity, and the time above this threshold or the “VEGF-suppression duration” in turn is governed by initial concentration, elimination half-life, and threshold level.¹⁰

Mathematical models are frequently used to analyze, characterize, or study PK and PK/PD relationships, and model-informed drug development is increasingly becoming an integral part of drug research.¹¹ This report uses modeling and simulations to investigate the vitreous PK of IVT-AFL, IVT-BRO, and IVT-RAN to quantitatively evaluate the effects of molar drug load, vitreous half-life, and binding affinity on the durability of drug action. We compared vitreous drug concentration-time profiles with aqueous VEGF suppression times per drug and visual acuity data from recent clinical trials with IVT-AFL and IVT-BRO in patients with choroidal neovasculariza-

tion secondary to age-related macular degeneration (nAMD).

Methods

Model Development

A linear, one compartment model was used to describe drug elimination from the vitreous. Molar drug concentrations were calculated based on drug dose. Molecular weight and parameter values used as a basis for simulations are summarized from published literature (Table 1).^{2–5,7,8,12–22} Initial vitreous molar drug concentrations were based on a vitreous volume of 4 mL and clinical doses of 2 mg for IVT-AFL, 6 mg for IVT-BRO, and 0.5 mg for IVT-RAN. Flip-flop PK relationships for each agent were assumed, consistent with Hutton-Smith et al.²³ and Caruso et al.,²⁴ with aqueous \approx vitreous half-life for IVT-AFL and IVT-RAN, and serum \approx vitreous half-life for IVT-BRO.

Macromolecules such as the anti-VEGF agents are largely cleared from the vitreous through the aqueous, then via the systemic circulation. “Flip-flop PK” means that a drug exits the vitreous and thus enters the aqueous (or the blood stream) at a slower rate than it is eliminated from the aqueous (or the blood stream). Under these conditions, the kinetics are dominated by the slower process (i.e., exit from the vitreous humor), which reveals the intravitreal elimination rate as measured in the aqueous (for IVT-AFL and IVT-RAN) or in the serum (for IVT-BRO). The resulting intravitreal PK corresponds to first-order elimination kinetics, which is completely characterized by the initial drug concentration and drug half-life or elimination rate constant. Multiple dose simulations were generated using the superposition principle.

The vitreous half-lives selected for use in the model were 9.1 days for IVT-AFL, 5.1 days for IVT-BRO, and 7.2 days for IVT-RAN based on the literature (Table 2). Published data on aqueous VEGF-suppression duration for IVT-AFL⁵ and IVT-RAN¹⁷ were used to derive intraocular VEGF-suppression thresholds for these agents by plotting VEGF-suppression durations on the x -axis to graphically identify the associated simulated vitreous molar concentrations for each agent where the VEGF-suppression duration would cross the concentration–time profile. The VEGF-suppression thresholds for IVT-AFL and IVT-RAN provided the lower and upper vitreous molar concentration thresholds, respectively, between which the VEGF-suppression threshold for IVT-BRO would lie. From this, a VEGF-suppression duration range for IVT-BRO was derived on the basis

Table 1. Parameter Value Overview

Parameter	IVT-AFL	IVT-BRO	IVT-RAN
Labeled drug dose, mg	2 ²	6 ³	0.5 ⁴
Molecular weight, kDa	115 ^{18,19}	26 ^{18,19}	48 ^{18,19}
Initial molar concentration in the vitreous, mol/L	4.348×10^{-6}	5.770×10^{-5}	2.604×10^{-6}
VEGF ₁₆₅ binding affinity (K_D), pM*	0.5 ⁷	28 ⁸	46 ⁷
Serum half-life after IV administration in humans [†] , days	5–7 ²	0.24 (non-human primate 5.6 hours) ²¹	~0.5 (non-human primate 14–15.5 hours) ¹⁴ 0.09 (2 hours) ²⁰
Aqueous- and serum-derived estimates of vitreous half-life after IVT administration, days	9–11 ¹³	4.4–5.1 ^{12,15}	5.8–9 ^{16,20,22}
Representative vitreous half-life used in the model, days	9.1 ¹³	5.1 ¹⁵	7.2 ¹⁶
Aqueous VEGF suppression duration, days	71 ⁵	51 days (model estimate)	36 ¹⁷

IV, intravenous.

*A drug with a smaller dissociation constant (K_D) has a higher binding affinity for the ligand.

†Unless otherwise specified.

of the VEGF-suppression threshold, initial concentration and half-life. Additionally, the model incorporated a weighting factor using binding affinity (specifically, the equilibrium dissociation constants [K_D]) for each agent to assess a most likely estimate of IVT-BRO VEGF-suppression threshold and to further characterize and compare the associated VEGF-suppression thresholds and durations of IVT-AFL and IVT-RAN with IVT-BRO:

$$\text{VEGF} - \text{Suppression Threshold}_{\text{IVT-BRO}} = (\text{AR} * \text{VEGF} - \text{Suppression Threshold}_{\text{IVT-RAN}} + \text{VEGF} - \text{Suppression Threshold}_{\text{IVT-AFL}}) / (1 + \text{AR})$$

where the aspect ratio in the model (AR) = $(K_{D_IVT-BRO} - K_{D_IVT-AFL}) / (K_{D_IVT-RAN} - K_{D_IVT-BRO})$.

MATLAB (MathWorks Inc, Natick, MA, USA) was used for simulation and graphical analysis. PK/PD comparisons of vitreous molar drug concentrations and VEGF-suppression durations were examined for single doses of IVT-AFL, IVT-BRO, and IVT-RAN, and for multiple doses of IVT-AFL and IVT-BRO according to the dosing schedules used in OSPREY,²⁵ HAWK, and HARRIER,²⁶ and also for an example dosing schedule in which IVT-AFL dosing was matched to that of IVT-BRO.

Clinical Study Data

OSPREY was a phase 2 trial of 89 treatment-naïve patients with nAMD randomized 1:1 to receive IVT-BRO 6 mg or IVT-AFL 2 mg (Supplementary Fig.).²⁵

Both groups received three initial monthly doses and were then treated every eight weeks (q8w) up to and including week 32. Patients in the IVT-AFL group continued treatment q8w after week 32 (at weeks 40 and 48). Patients in the IVT-BRO group were treated at week 44, thus providing two cycles at 12-weekly intervals (q12w; from weeks 32 to 44, then weeks 44 to 56).

HAWK and HARRIER were similarly designed phase 3 trials of 1817 patients with nAMD randomized 1:1:1 to IVT-BRO 3 mg, IVT-BRO 6 mg, or IVT-AFL 2 mg (HAWK), or 1:1 to IVT-BRO 6 mg or IVT-AFL 2 mg (HARRIER).²⁶ Both groups received three initial monthly doses; thereafter patients in the IVT-AFL group received treatment q8w to week 96 (Supplementary Fig.). Patients in the IVT-BRO group received treatment q12w to week 96, adjusted to q8w if disease activity was present.

Visual acuity data from the OSPREY trial²³ were overlaid on the modeled multidose vitreous molar concentration versus time profile of each respective drug to elaborate on PK/PD versus clinical response relationships.

Results

Single-Dose PK Simulations After Intravitreal Dosing

A linear, one-compartment model was used to describe drug elimination from the vitreous humor of the eye, without target-mediated drug deposition (that

Table 2. Published Half-Lives and Rationale for Half-Life Used in the Model

Anti-VEGF	Aqueous	Published Half-Life	Description	Reference
Aflibercept	Aqueous	9.1 days (mean) 11 days (median)	Aqueous half-life in nAMD eyes after single IVT injection (n = 5). Serial sampling of aqueous humor from the eye and blood/plasma was conducted at baseline, 4 hours and days 1, 3, 7, 14, and 28.	Do et al. ¹³ <i>Retina</i> 2020;40:643–647.
Aflibercept	Systemic	11.4 days (mean)	Systemic half-life after three monthly IVT injections of aflibercept 2 mg (n = 39). Blood samples were collected at baseline, 3 hours after injection, and at days 1, 3, 7, and 28 after the first and third doses.	Avery et al. ²² <i>Retina</i> 2017;37:1847–1858.
Aflibercept	Systemic	5–7 days	Systemic half-life after IV administration (no other information provided)	EYLEA (aflibercept) injection, for intravitreal use (prescribing information) ² .

Selected aflibercept half-life for model: 9.1 days

Rationale for selection: Do et al.¹³ is the only publication that reports the aqueous half-life of aflibercept in nAMD patients. The mean was used (a conservative estimate, but consistent with using the mean for other anti-VEGF) and the median of 11 days was examined in sensitivity analyses. Half-life rank order is consistent with molecular weight rank order: aflibercept > ranibizumab > brolucizumab.

Brolucizumab	Systemic	5.1 days (geometric mean)	Systemic half-life after a single IVT injection (n = 68) of brolucizumab 0.5 mg (n = 1), 3.0 mg (n = 13), 4.5 mg (n = 26), or 6.0 mg (n = 28).	Holz et al. ¹⁵ <i>Ophthalmology</i> 2016;123:1080–1089.
Brolucizumab	Systemic	4.3 days (mean)	Systemic half-life after IVT injection (n = 42). Blood samples were collected at baseline and after 6, 24, 72, 168, 336, 504 and 672 hours.	ClinicalTrials.gov number, NCT02507388. ¹²
Brolucizumab	Systemic	4.4 days	Systemic half-life after a single IVT dose (no other information provided).	BEOVU (brolucizumab-dbl) injection, for intravitreal injection (prescribing information) ³
Brolucizumab	Systemic	5.6 hours	Systemic half-life after IV injection of brolucizumab (2.06±0.05 mg/kg) in non-human primates (n = 11).	Nimz et al. ²¹ <i>Invest Ophthalmol Vis Sci</i> 2016;57:4996–4996.

Selected brolucizumab half-life for model: 5.1 days

Rationale for selection: Vitreous half-life = serum half-life after IVT flip-flop PK assumption is supported (serum IVT half-life 4.5–5.1 days > estimated IV half-life of <0.25 days), with Holtz et al.¹⁵ estimate (5.1 days) providing the least conservative mean estimate of half-life using serum concentration versus time after IVT injection. Half-life rank order is consistent with molecular weight rank order: aflibercept > ranibizumab > brolucizumab.

Table 2. Continued

Anti-VEGF	Vitreous	Published Half-Life	Description	Reference
Ranibizumab	Vitreous	9 days (mean)	Vitreous half-life from population PK modeling of serum concentrations after single- and multiple-dosing of IVT ranibizumab 0.3–2 mg (n = 674)	Xu et al. ²⁰ <i>Invest Ophthalmol Vis Sci</i> 2013;54:1616–1624.
Ranibizumab	Aqueous	7.19 days (mean)	Aqueous half-life in non-vitreotomized eyes (n = 15) after a single IVT injection of ranibizumab 0.5 mg. An aqueous humor sample was obtained during cataract surgery between 1 and 37 days after injection.	Krohne et al. ¹⁶ <i>Am J Ophthalmol</i> 2012;154:682–686.
Ranibizumab	Systemic	5.8 days (mean)	Systemic half-life after three monthly doses of IVT ranibizumab 0.5 mg (n = 43). Blood samples were collected at baseline, 3 hours after injection, and at days 1, 3, 7, and 28 after the first and third doses.	Avery et al. ²² <i>Retina</i> 2017;37:1847–1858.
Ranibizumab	Systemic	0.09 days (mean) (2 hours)	Systemic IV half-life estimated from population PK modeling of single- and multiple-dosing of IVT ranibizumab.	Xu et al. ²⁰ <i>Invest Ophthalmol Vis Sci</i> 2013;54:1616–1624.
Ranibizumab	Systemic	<0.25 days in non-human primate	Half-life after single doses of IV ranibizumab 1 or 4 mg (n = 8). Blood samples were collected at baseline and after 5, 15, and 30 minutes, hourly from 1 to 10 hours; and at 16, 24, 36, and 48 hours.	Gaudreault et al. ¹⁴ <i>Invest Ophthalmol Vis Sci</i> 2005;46:726–733.

Selected ranibizumab half-life for model: 7.2 days

Rationale for selection: Half-life rank order is consistent with molecular weight rank order: aflibercept > ranibizumab > brodalumab. Krohne et al.¹⁶ estimate of 7.19 days is consistent with IVT-AFL VEGF suppression 2-times longer than ranibizumab. Xu et al.²⁰ data (half-life of 9 days) are inconsistent with other data and used sparse sampling PK from single- and multiple-dose studies of a range of ranibizumab doses (0.3, 0.5, and 2 mg). However, these data were used within the sensitivity analysis of ranibizumab.

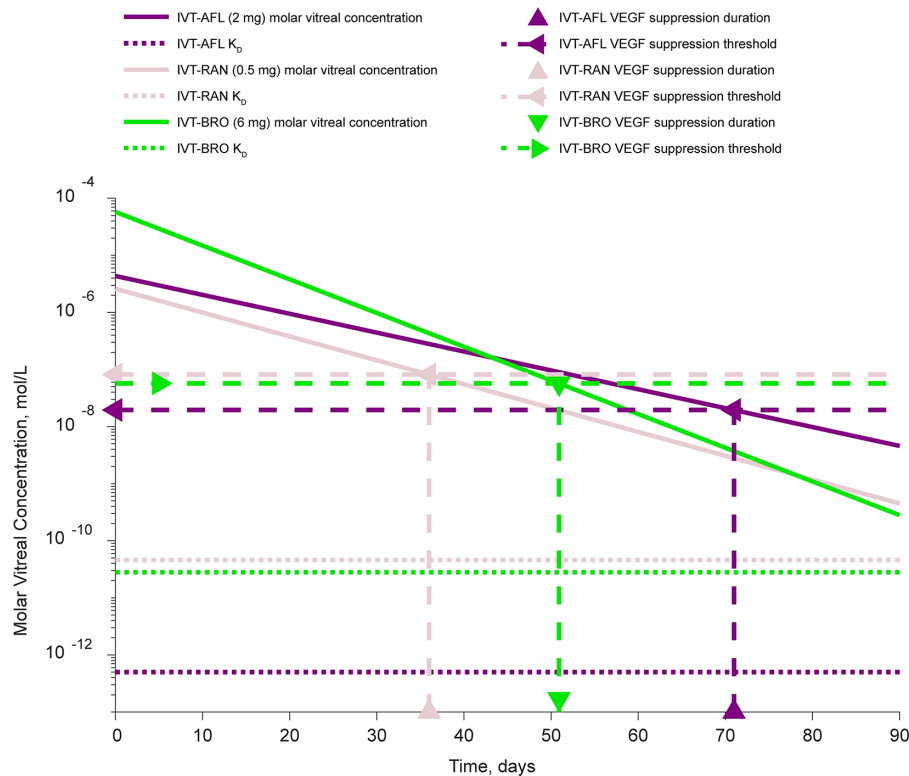


Figure 1. Vitreous PK simulations, VEGF-suppression thresholds, and VEGF-suppression durations for single-dose IVT-AFL, IVT-BRO, and IVT-RAN. *Thick solid lines* are vitreous molar concentrations based on representative half-lives and translate into representative VEGF-suppression thresholds (*horizontal thick dashed lines*) and VEGF-suppression durations (*vertical thick dashed lines*). K_D values are shown as *thick dotted lines*.

is, excluding PK of the drug–ligand complex). Resulting vitreous PK corresponded to first-order elimination kinetics, which were completely characterized by initial drug concentrations and drug half-life or elimination rate constant, yielding an exponential decay (Fig. 1).

As shown on the semilogarithmic scale, vitreous molar concentrations after IVT-BRO peaked (C_{max}) higher and decreased more quickly to trough (C_{min}) compared with IVT-AFL, consistent with their relative molar doses and representative vitreous half-lives of 5.1 and 9.1 days, respectively, estimated using serum PK for IVT-BRO and aqueous PK for IVT-AFL. On the basis of the model, it was estimated that vitreous molar concentrations of IVT-BRO and IVT-AFL were approximately equal by day 43 after a single intravitreal dose, and thereafter IVT-BRO levels were lower. The vitreous molar concentrations after IVT-RAN were lower than those of IVT-AFL throughout the 90-day simulation period and were higher than those of IVT-BRO after day 78. Vitreous molar concentrations of IVT-AFL were sufficient to effectively suppress VEGF through day 71 (compared with 36 days for IVT-RAN); however, the molar concentration of IVT-BRO is, on average, no longer sufficient to effectively suppress VEGF beyond day 51.

Because ranges of half-lives are published in the literature, model parameters were modified accordingly (Fig. 2). Retaining the same VEGF-suppression durations, the model shows the effects of using the upper and lower limits of the half-lives for IVT-AFL (Fig. 2A) and IVT-RAN (Fig. 2C) on the vitreous molar concentrations and, consequently, the VEGF-suppression thresholds. For IVT-BRO, the model shows the effect of modifying the VEGF-suppression threshold point estimate toward that of IVT-RAN (upper boundary) or IVT-AFL (lower boundary). The representative VEGF-suppression duration estimated for IVT-BRO was 51 days. The minimum of the estimated range of the IVT-BRO VEGF-suppression duration, in which adequate drug concentrations higher than the suppression threshold are maintained, was calculated to be 48 days, and the maximum suppression duration was estimated to be 59 days with the 5.1 days vitreous half-life parameter in the model (Fig. 2B). Assuming shorter (corresponding to the half-life reported in the label) versus longer half-life intervals ranging from 4.4 to 5.1 for IVT-BRO and therefore higher versus lower suppression thresholds, the estimated suppression duration range was 37 to 59 days. Weighting factors based on ratios of binding

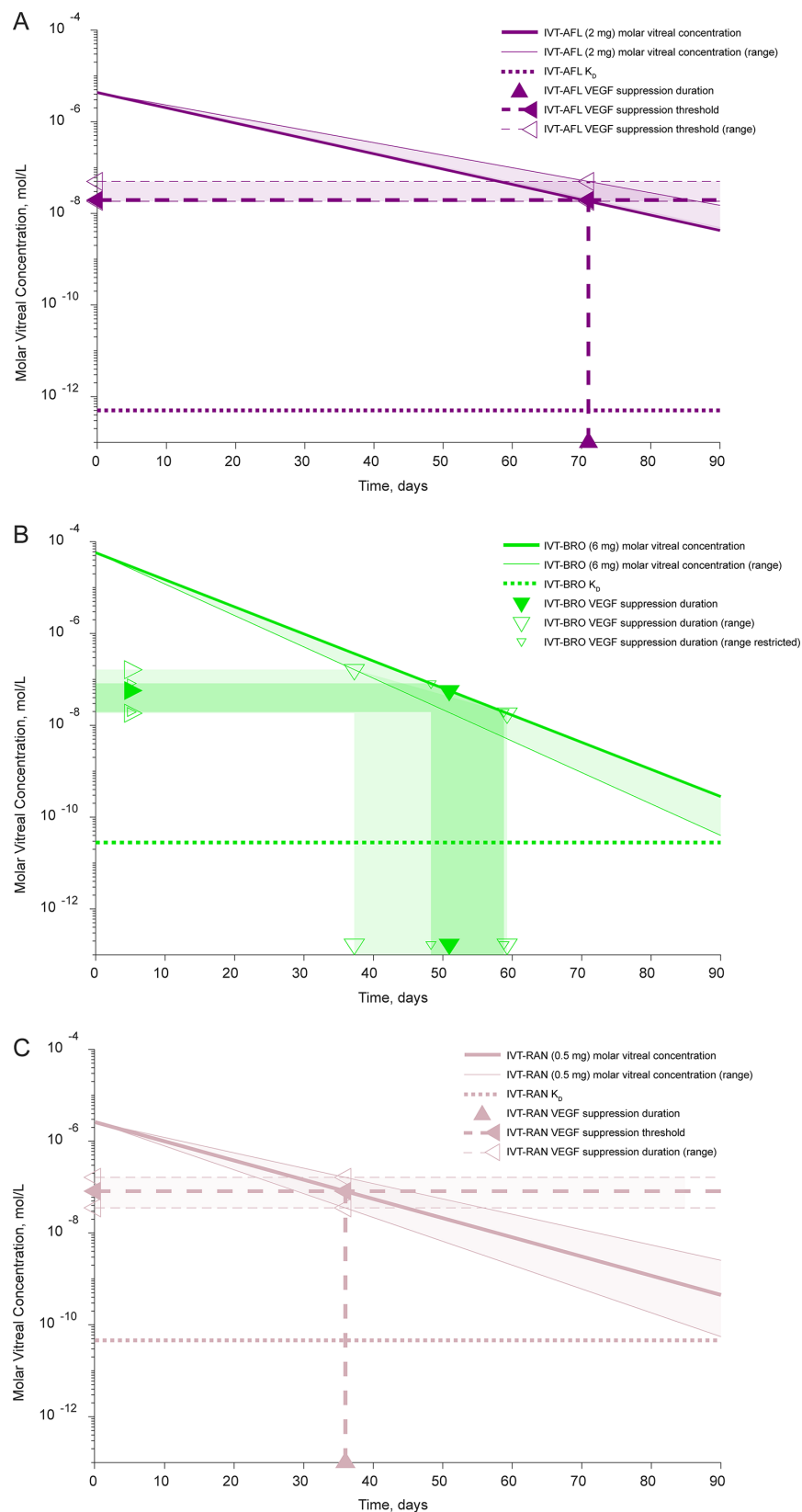


Figure 2. Vitreous PK simulation uncertainty showing impact on VEGF-suppression thresholds and durations for single-dose (A) IVT-AFL, (B) IVT-BRO, and (C) IVT-RAN. *Thick solid lines* are vitreous molar concentrations based on representative half-lives and translate into representative VEGF-suppression thresholds (*thick horizontal dashed lines*) as depicted in Figure 1. Shaded areas framed by *thin solid lines* are based on reported half-life time ranges and, with given VEGF-suppression durations, translate into ranges for estimated VEGF-suppression thresholds. Resulting range estimates for IVT-BRO in *light green shades* result from ranges and *dark green shades* from point estimates for IVT-AFL and IVT-RAN.

affinities of the drugs had a negligible contribution to the VEGF suppression duration estimates in the model.

Multiple-dose PK Simulations After Intravitreal Dosing

Multiple dosing simulations based on the OSPREY posology showed wider fluctuation between vitreous molar C_{\max} and C_{\min} for IVT-BRO than with IVT-AFL (Fig. 3A). With IVT-AFL administered q8w after three initial monthly doses, vitreous molar concentrations were maintained above the VEGF-suppression threshold to week 56, and gains/improvements in visual acuity were maintained (Fig. 3B). With IVT-BRO, C_{\min} was below the intraocular VEGF-suppression threshold during the q12w phase from week 40 onward to week 56, and a decrease in best-corrected visual acuity (BCVA) gains was observed (Fig. 3C).

Figure 3D shows simulations of vitreous molar concentrations after a modified dosing schedule to allow for matched dosing of IVT-AFL and IVT-BRO q12w after week 32 based on the VEGF-suppression duration of 71 days for IVT-AFL and 51 days for IVT-BRO. The modeling also incorporated the very minor accumulation applicable in the multiple-dose setting. During the matched q12w dosing scenario for both agents, the molar vitreous concentrations of IVT-BRO fell below the respective VEGF-suppression threshold for more than two times longer than those for IVT-AFL (Fig. 3D).

Similarly, simulations based on the HAWK/HARRIER dosing schedule showed that IVT-BRO vitreous molar concentrations rapidly fell below the effective VEGF-suppression threshold and below IVT-AFL molar concentrations once the q12w dosing schedule was initiated after week 16 (Fig. 4). With IVT-AFL, vitreous molar concentrations remained above the VEGF-suppression threshold throughout the study to week 96. In HAWK/HARRIER, only 39% to 45% of the total study population who received IVT-BRO were maintained at a q12w dosing regimen through week 96, because patients who experienced a five or more letter decrease in BCVA were switched to q8w dosing.

Discussion

Current treatment strategies for anti-VEGF agents include dosing at fixed intervals, treat-and-extend (T&E), or *pro re nata* (as needed; PRN), which were evaluated in clinical trials including ANCHOR

and MARINA (q4w dosing), PRONTO (PRN), and HARBOR for IVT-RAN (PRN compared with q4w dosing); VIEW 1 and VIEW 2 for IVT-AFL (q8w dosing in year 1; capped q12w PRN in year 2); and HAWK and HARRIER for IVT-BRO (q12w dosing).⁶ Because PRN dosing can lead to undertreatment in clinical practice, T&E dosing has become a popular treatment strategy to reduce the treatment burden associated with fixed dosing. For IVT-AFL, T&E dosing was evaluated during the first and second years of treatment in ARIES and ALTAIR (after three initial monthly doses).^{27,28} The obvious challenge of extending the treatment interval is ensuring that intraocular (i.e., vitreous) molar concentrations of the anti-VEGF agent are sufficient to reduce excessive VEGF receptor signaling by preventing binding of VEGF ligands to the VEGF receptors. Because previous studies have investigated the aqueous VEGF-suppression durations for IVT-AFL^{5,29} and IVT-RAN,^{17,29} but not IVT-BRO, our analysis explored this using well-established PK/PD modeling principles.

Because all anti-VEGF agents are administered in molar concentrations many-fold higher than the target VEGF concentrations in the eye, all initially inhibit VEGF completely.⁹ However, because vitreous half-lives of macromolecules (or biologicals) are generally proportional to their molecular masses (IVT-AFL > IVT-RAN > IVT-BRO), a larger anti-VEGF drug would have a longer elimination half-life. These attributes of IVT-AFL coupled with a higher VEGF binding affinity would be expected to yield a longer VEGF-suppression duration.

Published data on VEGF-suppression durations for IVT-AFL^{5,29} and IVT-RAN^{17,29} allow the calculation of VEGF-suppression thresholds for these agents. Using these thresholds and reported values for binding affinity, the current model was used to calculate a representative VEGF-suppression duration for IVT-BRO. Although reported dissociation constants are orders of magnitude smaller for IVT-AFL than for IVT-RAN and IVT-BRO, the calculated VEGF-suppression thresholds are relatively close, indicating that in vitro binding affinity differences may not quantitatively translate directly into in vivo inhibition. This is likely because of differences in physical-chemical conditions and target turnover. However, the rank order for IVT-AFL and IVT-RAN is consistent for the binding affinities of the agents and their VEGF-suppression thresholds, providing the rationale for the binding-affinity weighting that was used to derive representative values for the IVT-BRO VEGF-suppression threshold.

There are some inherent limitations in our model, and where possible we have attempted to minimize their

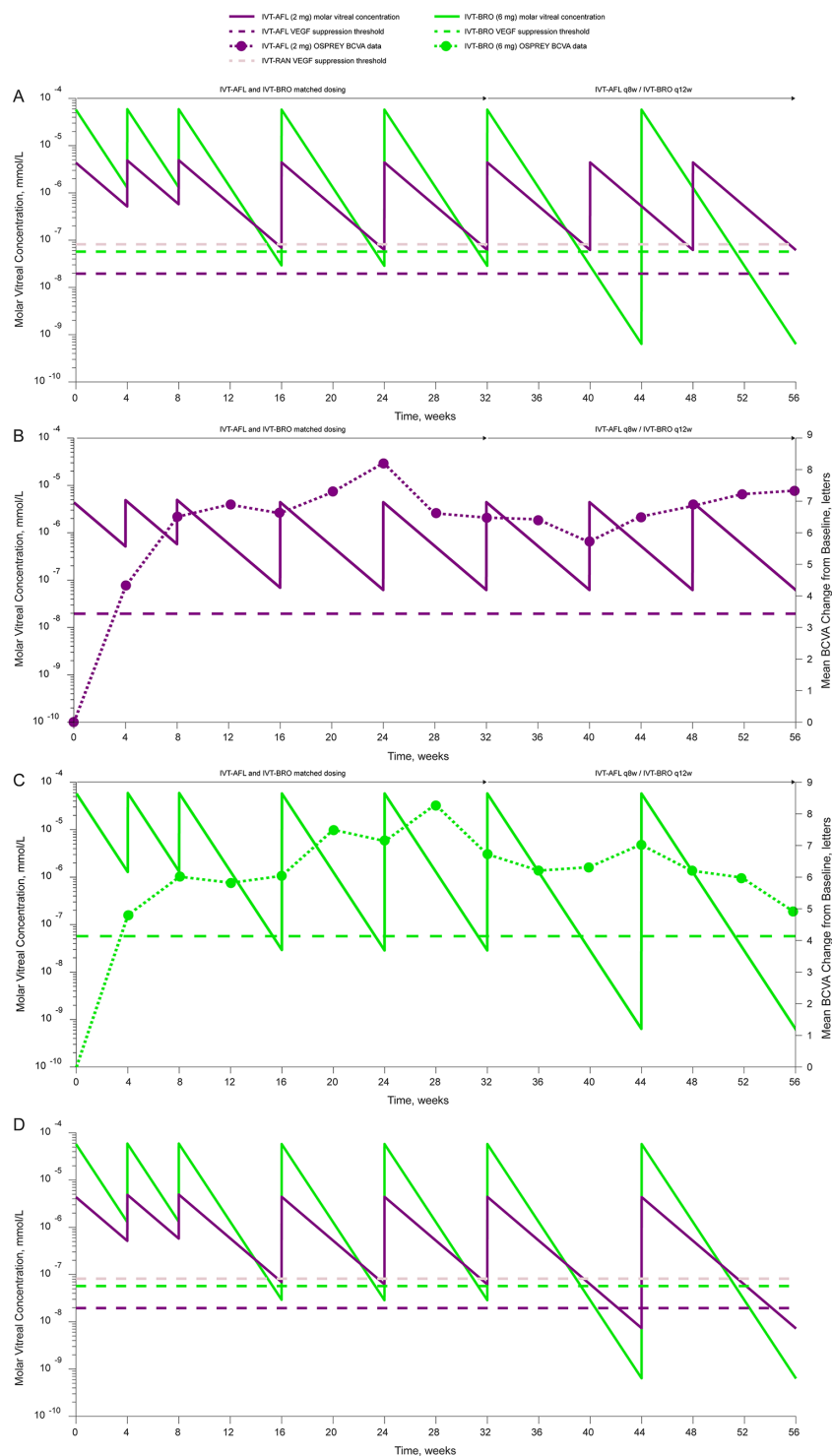


Figure 3. Vitreous PK simulations based on OSPREY dosing and (A,B) VEGF-suppression thresholds for IVT-AFL and (A,C) IVT-BRO, and (B,C) showing changes in BCVA and (D) vitreous PK simulations and VEGF-suppression thresholds based on IVT-AFL and IVT-BRO-matched q12w dosing after week 32. *Thick solid lines* are vitreous molar concentrations based on representative half-lives and translate into representative VEGF-suppression thresholds (*thick horizontal dashed lines*). BCVA data are shown as *dotted lines*.

impact. Indeed, any shortcomings in the published PK parameter estimates used (such as missing initial, intermediate, or terminal phase samples) will be propagated to the PK parameter estimates. Caruso et al.²⁴

performed a model-based meta-analysis to determine consensus values for the intraocular half-lives of IVT-AFL, IgG antibodies, Fab fragments, and IVT-BRO. Consistent with this, in our model, intravitreal drug

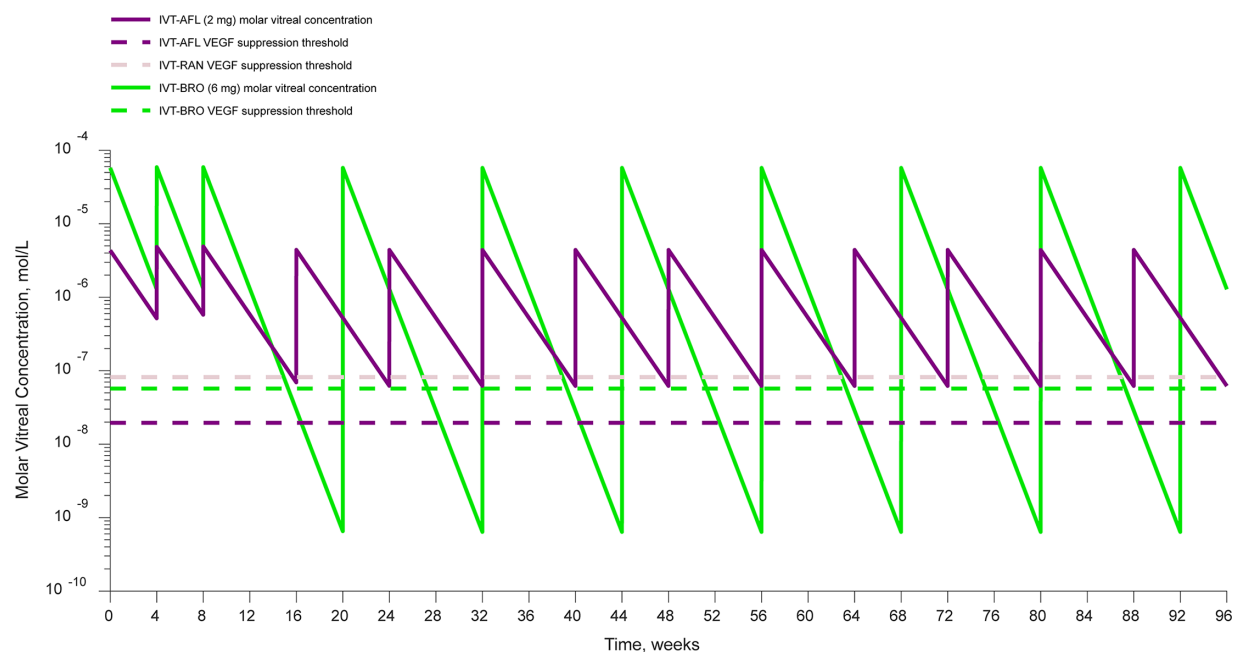


Figure 4. Vitreous PK simulations based on HAWK and HARRIER dosing and VEGF-suppression thresholds for IVT-AFL and brolucizumab. Thick solid lines are vitreous molar concentrations based on representative half-lives and translate into representative VEGF-suppression thresholds (thick horizontal dashed lines).

half-lives have been estimated from serum/plasma and aqueous sampling. Although the true relationship between PK in the vitreous, aqueous, and serum has not been fully characterized, we can use a concept called “flip-flop” kinetics to support the selection of published drug half-life parameters used in the model.^{23,24} Our model also assumes serum \approx vitreous half-life for IVT-BRO and aqueous \approx vitreous half-life for IVT-AFL because these have been proposed as valid surrogates on the basis of this principle.²⁴

Target-mediated drug disposition is the phenomenon in which a drug binds with high affinity to its pharmacological target (in this case the VEGF ligand) to such an extent that this affects its PK characteristics. It is a saturable clearance mechanism for biologics, but here the current one-compartment model excluded target-mediated disposition and clearance effects because these are usually not relevant when the concentration of the drug is higher than the concentration of the target. These factors only play a role when drug concentrations approach that of the target. Our subsequent comparisons with the reported clinical effects of the anti-VEGF agents further support the appropriateness of our approach, despite its simplicity.

We acknowledge that the uncertainty regarding a specific half-life estimation propagates to the respective VEGF-suppression thresholds. Because the VEGF-

suppression threshold and duration for IVT-BRO have been estimated from the VEGF-suppression threshold for IVT-AFL and IVT-RAN, any uncertainty continues into the estimation of these parameters for IVT-BRO. The modeling shows the effects of this uncertainty using the lower and upper limits of the IVT-BRO VEGF-suppression threshold on the estimated VEGF-suppression duration. Additionally, the half-lives are average values for the studies and, at a patient level, half-lives will vary between individuals leading to a potentially wide range of half-life values and VEGF-suppression durations within a patient population. Future analyses modeling the proportion of patients with different VEGF suppression durations would also be of value.

The molecular weight of IVT-BRO results in the shortest half-life of the three anti-VEGF agents; however, the high initial drug concentration partially compensates for the faster elimination. In the current model, using the half-life for IVT-BRO reported in the prescribing information (4.4 days)³ rather than the 5.1 days from the medical literature, the corresponding time point at which the IVT-BRO molar vitreous concentrations decreased to levels approximately equal to those of IVT-AFL changed from approximately 43 days to approximately 32 days. Accordingly, the estimated VEGF-suppression durations for IVT-BRO also decreased from an average of 51 days to

Table 3. Trials of IVT-AFL or IVT-BRO Reporting Patients Achieving q12w Dosing at Two Years

~2 Year nAMD Phase 3 Trials	Treatment Arm	Dose Regimens	Proportion (%) of Patients With Treatment Interval Extended to \geq q12 Weeks	Proportion (%) of Patients With Treatment Interval Extended to \geq q16 Weeks
HAWK*	6 mg IVT-BRO	q12w fixed; failures drop to q8w fixed through 96 weeks	45.4	Not reported
	2 mg IVT-AFL	q8w fixed without option to extend	Not studied	Not studied
HARRIER*	6 mg IVT-BRO	q12w fixed; failures drop to q8w fixed through 96 weeks	38.6	Not reported
	2 mg IVT-AFL	q8w fixed without option to extend	Not studied	Not studied
VIEW 1/2†	IVT-AFL q4w	q4w fixed in year 1 then capped PRN through year 2	53.9	Not reported
	IVT-AFL q8w	q8w fixed in Year 1 then capped PRN through year 2	47.9	Not reported
ALTAIR‡	IVT-AFL q2w T&E	T&E with extensions by 2-weekly intervals	56.9	41.5
	IVT-AFL q4w T&E	T&E with extensions by 4-weekly intervals	60.2	46.3
ARIES§	IVT-AFL early T&E	T&E early (within first year)	47.2	30.2
	IVT-AFL late T&E	T&E late (after first year)	51.9	26.9

*HAWK/HARRIER^{3,26}: Patients in the IVT-BRO 6 mg arm received 3 initial monthly doses, then IVT-BRO 6 mg q8w through week 16, then q12w for those meeting prespecified criteria, with others remaining on q8w dosing; patients meeting disease activity criteria in the q12w arm dropped to q8w. Patients in the IVT-AFL arms in these trials received fixed q8w 2 mg dosing with no option for extension. HARRIER included a 3 mg IVT-BRO dose group; this is not in scope for this analysis and is not included.

†VIEW³⁰: Patients received IVT-RAN 0.5 mg q4w or IVT-AFL 2 mg q4w or IVT-AFL 2 mg q8w after three initial monthly doses for the first year, with capped PRN after year 1 through year 2. VIEW included a 0.5 mg IVT-AFL dose group; this is not in scope for this analysis and is not included.

‡ALTAIR²⁷: Patients received IVT-AFL 2 mg as three initial monthly doses followed by q8w. From week 16, patients meeting criteria extended intervals by either 2-week or 4-week adjustments.

§ARIES²⁸: Patients received IVT-AFL 2 mg as three initial monthly doses followed by q8w. Patients in the early T&E arm could extend IVT-AFL 2 mg treatment intervals by 2-week extensions from week 16. Patients in the late T&E arm received IVT-AFL 2 mg q8w through week 52, with intervals thereafter extended by two-week adjustments.

44 days. This shows that the elimination half-life of respective molecules contributes largely towards the potential durability profile of each agent.

Despite the acknowledged limitations, our modeling approach is consistent with those of other groups. Relative to IVT-RAN VEGF suppression activity after 30 days, Stewart and Rosenfeld¹⁰ calculated that similar

VEGF suppression activity would occur with IVT-AFL 0.5, 1.15, 2, and 4 mg after 73, 79, 83, and 87 days, respectively. Fauser et al.⁵ measured VEGF-A levels in 27 patients with nAMD, collecting a total of 132 aqueous humor specimens before and after IVT-AFL administration, and established that the mean VEGF-suppression duration below the lower limit of

VEGF quantification (<4 pg/mL) was >71 (± 18) days. In a separate study of 89 patients with nAMD, the extended VEGF-suppression duration with IVT-AFL versus IVT-RAN translated into a twofold decrease in clinical activity of choroidal neovascularization as measured using spectral domain optical coherence tomography.²⁹ Muether et al.¹⁷ measured VEGF in the aqueous humor of 38 patients with nAMD treated with IVT-RAN and estimated the VEGF-suppression duration to be 36 days.

In the current analysis, the OSPREY trial, a head-to-head comparison of IVT-BRO and IVT-AFL, was used to examine simulated vitreous molar drug concentrations with BCVA data.²⁵ With IVT-AFL q8w after three initial monthly doses, the vitreous molar drug concentrations remained above the calculated VEGF-suppression threshold throughout the study and gains in BCVA were maintained to week 48.²⁵ IVT-BRO molar drug concentrations were calculated to fall slightly below the estimated VEGF-suppression threshold toward the end of each q8w dosing period. When the IVT-BRO dosing was extended to q12w, molar drug concentrations dropped further below the estimated VEGF-suppression threshold, where they remained for longer periods of time. These prolonged drops may have been clinically relevant because the overall BCVA gains decreased when the IVT-BRO concentrations remained below the VEGF-suppression threshold during the q12w extensions. The prescribing recommendation for IVT-BRO is 6 mg monthly for the first three doses, followed by one dose of 6 mg every eight to 12 weeks (~ 56 –84 days).³ Given the potential loss of effective VEGF suppression with IVT-BRO after day 48 to 59 or even as early as 37 days as determined by our model, caution might be recommended before extending dosing intervals beyond these timeframes.

It is not possible to perform a similar comparison of PK levels and functional outcomes using published data from HAWK and HARRIER because of the study designs. In both trials, IVT-AFL was injected with fixed q8w intervals but IVT-BRO was injected q8w or q12w depending on functional and anatomic measures of disease activity.²⁶ The available q12w-only BCVA data do not reflect the total population because poor responders were removed from the q12w dosing groups in the pivotal trials.²⁶ Relevant large-scale studies where q12w or longer treatment intervals were reported up to two years for IVT-AFL or IVT-BRO are shown in Table 3. The proportion of patients maintaining q12w dosing with IVT-BRO after the three initial monthly doses in HAWK and HARRIER was 56% and 50% through week 48, and 45% and 39% through week 96, respectively.^{3,26} In comparison, by

week 96 of the pivotal VIEW trials, 48% to 54% of patients treated with IVT-AFL were maintained on q12w dosing.³⁰ In the ALTAIR and ARIES trials, by the end of year 2 (weeks 96 and 104, respectively), $\sim 47\%$ to 60% of patients were treated with ≥ 12 -week IVT-AFL treatment intervals and $\sim 27\%$ to 46% were treated every 16 weeks.²⁷ These data suggest that on average, higher proportions of subjects would be treated with q12w or longer intervals with IVT-AFL than with IVT-BRO. This assessment is based on indirect comparisons of the agents with different dosing regimens per agent.

Overall, the VEGF-suppression durations after single intravitreal doses can be ranked as IVT-AFL (71 days)⁵ $>$ IVT-BRO (approximately 51 days [model derived]) $>$ IVT-RAN (36 days),¹⁷ which is consistent with the molecular characteristics of the anti-VEGF agents and their associated vitreous PK after intravitreal injection. The PK/PD modeling indicates that this behavior is preserved for multiple-dosing scenarios and provides a possible rationale for the differences in functional outcomes observed in clinical trials of IVT-AFL and IVT-BRO, and in the proportion of patients who can successfully be maintained on a q12w dosing schedule.

Acknowledgments

The authors thank Samia Ezzine (Bayer) for PK/PD expertise, extensive discussions regarding intraocular PK/PD, and early concept discussions; Todd Katz (formerly of Bayer) for early concept discussions; Joachim Hoechel, Sergio Leal, Joerg Lippert, and Walter Schmitt (all Bayer) for critical comments on the work; and Sarah Feeny of ApotheCom (London, UK) for medical writing and editorial assistance.

Supported by Bayer Consumer Care, AG, Pharmaceuticals, Basel, Switzerland.

Disclosure: **T. Eissing**, Bayer AG (E); **M.W. Stewart**, Allergan (F), Kanghong (F), Regeneron (F), Alkermest (C), Bayer (C); **C.X. Qian**, Allergan (C), Bausch & Lomb (C), Bayer (C), Knight Therapeutics (C), Novartis (C); **K.D. Rittenhouse**, Bayer Consumer Care AG (E)

References

1. Aiello LP, Avery RL, Arrigg PG, et al. Vascular endothelial growth factor in ocular fluid of patients

- with diabetic retinopathy and other retinal disorders. *N Engl J Med*. 1994;331:1480–1487.
2. Bayer Pharma AG. Eylea (aflibercept solution for injection) summary of product characteristics. 2020.
 3. Novartis. BEOVU (brolucizumab-dblb) injection, for intravitreal injection [prescribing information]. 2019.
 4. Novartis. LUCENTIS (ranibizumab injection) for intravitreal injection [prescribing information]. 2018.
 5. Fauser S, Schwabecker V, Muether PS. Suppression of intraocular vascular endothelial growth factor during aflibercept treatment of age-related macular degeneration. *Am J Ophthalmol*. 2014;158:532–536.
 6. Khanna S, Komati R, Eichenbaum DA, Hariprasad I, Ciulla TA, Hariprasad SM. Current and upcoming anti-VEGF therapies and dosing strategies for the treatment of neovascular AMD: a comparative review. *BMJ Open Ophthalmol*. 2019;4:e000398.
 7. Papadopoulos N, Martin J, Ruan Q, et al. Binding and neutralization of vascular endothelial growth factor (VEGF) and related ligands by VEGF Trap, ranibizumab and bevacizumab. *Angiogenesis*. 2012;15:171–185.
 8. Gaudreault J, Gunde T, Floyd HS, et al. Preclinical pharmacology and safety of ESBA1008, a single-chain antibody fragment, investigated as potential treatment for age related macular degeneration. *Invest Ophthalmol Vis Sci*. 2012;53:3025.
 9. Hsu M-Y, Hung Y-C, Hwang D-K, et al. Detection of aqueous VEGF concentrations before and after intravitreal injection of anti-VEGF antibody using low-volume sampling paper-based ELISA. *Sci Rep*. 2016;6:34631.
 10. Stewart MW, Rosenfeld PJ. Predicted biological activity of intravitreal VEGF Trap. *Br J Ophthalmol*. 2008;92:667–668.
 11. Marshall S, Burghaus R, Cosson V, et al. Good practices in model-informed drug discovery and development: practice, application, and documentation. *CPT: Pharmacometrics Syst Pharmacol*. 2016;5:93–122.
 12. ClinicalTrials.gov. Safety and pharmacokinetics of RTH258 in subjects with age-related macular degeneration. NCT02507388.
 13. Do DV, Rhoades W, Nguyen QD. Pharmacokinetic study of intravitreal aflibercept in humans with neovascular age-related macular degeneration. *Retina*. 2020;40:643–647.
 14. Gaudreault J, Fei D, Rusit J, Suboc P, Shiu V. Preclinical pharmacokinetics of ranibizumab (rhFabV2) after a single intravitreal administration. *Invest Ophthalmol Vis Sci*. 2005;46:726–733.
 15. Holz FG, Dugel PU, Weissgerber G, et al. Single-chain antibody fragment VEGF inhibitor RTH258 for neovascular age-related macular degeneration: a randomized controlled study. *Ophthalmology*. 2016;123:1080–1089.
 16. Krohne TU, Liu Z, Holz FG, Meyer CH. Intraocular pharmacokinetics of ranibizumab following a single intravitreal injection in humans. *Am J Ophthalmol*. 2012;154:682–686.
 17. Muether PS, Hermann MM, Droge K, Kirchhof B, Fauser S. Long-term stability of vascular endothelial growth factor suppression time under ranibizumab treatment in age-related macular degeneration. *Am J Ophthalmol*. 2013;156:989–993.
 18. Noble J. Recent advances in the management of age-related macular degeneration: What to expect over the next few years. A report from the 2017 Annual Meeting of the American Academy of Ophthalmology (AAO). *Ophthalmol Sci Update*. 2017.
 19. Stewart MW. Extended duration vascular endothelial growth factor inhibition in the eye: failures, successes, and future possibilities. *Pharmaceutics*. 2018;10:21.
 20. Xu L, Lu T, Tuomi L, et al. Pharmacokinetics of ranibizumab in patients with neovascular age-related macular degeneration: a population approach. *Invest Ophthalmol Vis Sci*. 2013;54:1616–1624.
 21. Nimz EL, Van't Land CW, Yáñez JA, Chastain JE. Intraocular and systemic pharmacokinetics of brolucizumab (RTH258) in nonhuman primates. *Invest Ophthalmol Vis Sci*. 2016;57:4996.
 22. Avery RL, Castellarin AA, Steinle NC, et al. Systemic pharmacokinetics and pharmacodynamics of intravitreal aflibercept, bevacizumab, and ranibizumab. *Retina*. 2017;37:1847–1858.
 23. Hutton-Smith LA, Gaffney EA, Byrne HM, Maini PK, Gadkar K, Mazer NA. Ocular pharmacokinetics of therapeutic antibodies given by intravitreal injection: estimation of retinal permeabilities using a 3-compartment semi-mechanistic model. *Mol Pharm*. 2017;14:2690–2696.
 24. Caruso A, Futh M, Alvarez-Sanchez R, et al. Ocular half-life of intravitreal biologics in humans and other species: meta-analysis and model-based prediction. *Mol Pharm*. 2020;17:695–709.
 25. Dugel PU, Jaffe GJ, Sallstig P, et al. Brolucizumab versus aflibercept in participants with neovascular age-related macular degeneration: a randomized trial. *Ophthalmology*. 2017;124:1296–1304.

26. Dugel PU, Koh A, Ogura Y, et al. HAWK and HARRIER: phase 3, multicenter, randomized, double-masked trials of brolucizumab for neovascular age-related macular degeneration. *Ophthalmology*. 2020;127:72–84.
27. Ohji M, Takahashi K, Okada AA, et al. Efficacy and safety of intravitreal aflibercept treat-and-extend regimens in exudative age-related macular degeneration: 52- and 96-week findings from ALTAIR. *Adv Ther*. 2020;37:1173–1187.
28. Mitchell P, Holz FG, Hykin P, et al. Efficacy and safety of intravitreal aflibercept using a treat-and-extend regimen for neovascular age-related macular degeneration: the ARIES study [published online ahead of print March 22, 2021]. *Retina*. <https://doi.org/10.1097/IAE.0000000000003128>.
29. Fauser S, Muether PS. Clinical correlation to differences in ranibizumab and aflibercept vascular endothelial growth factor suppression times. *Br J Ophthalmol*. 2016;100:1494–1498.
30. Khurana RN, Rahimy E, Joseph WA, et al. Extended (every 12 weeks or longer) dosing interval with intravitreal aflibercept and ranibizumab in neovascular age-related macular degeneration: post hoc analysis of VIEW trials. *Am J Ophthalmol*. 2019;200:161–168.